Protective Effects of Lactobacillus reuteri SJ-47 Exopolysaccharides on Human Skin Fibroblasts Damaged by UVA Radiation

Jingsha Zhao
Beijing Technology and Business University
Hao Fu
Beijing Technology and Business University
Yongtao Zhang
Beijing Technology and Business University
meng li (limeng@btbu.edu.cn)
Beijing Technology and Business University https://orcid.org/0000-0002-7354-6480
Dongdong Wang
Beijing Technology and Business University
Dan Zhao
Beijing Technology and Business University
Jiachan Zhang
Beijing Technology and Business University
Changtao Wang
Beijing Technology and Business University

Research Article

Keywords: Lactobacillus reuteri SJ-47 exopolysaccharides, skin photoaging, oxidative stress

Posted Date: August 22nd, 2022

DOI: https://doi.org/10.21203/rs.3.rs-1958828/v1

Abstract

Ultraviolet rays in sunlight can cause skin damage and premature aging. This study demonstrates that *Lactobacillus reuteri* SJ-47 exopolysaccharides (EPS) protect human skin fibroblasts (HSF) under UVA radiation. During the course of the experiments, we investigate the oxidative stress protection and anti-aging effects of exopolysaccharides on HSF at the biochemical, cellular and molecular levels. The results show that EPS can increase the antioxidant capacity of cells, decrease the amount of reactive oxygen species (ROS) and malondialdehyde (MDA), while improve the expression of antioxidant enzymes. At the same time, EPS can increase collagen content, which can effectively regulate the expression of genes in the senescence and apoptosis pathways, and delay skin photoaging caused by UVA irradiation.

1. Introduction

The skin is the main organ that wraps the surface of the human body and protects it from external harm and damage [1]. Skin aging is a progressive change in the physiology and appearance of the skin caused by the accumulation of endogenous and exogenous factors [2]. As the skin ages, its protective barrier is damaged. The natural aging of the skin is a gradual process, but exogenous factors can accelerate it, among which ultraviolet rays from the sun are an important external factor that triggers premature skin aging [3]. Ultraviolet light can be divided into three categories according to wavelength: UVA, UVB and UVC [3]. UVA has a strong penetrating ability. It triggers endogenous photosensitization due to its penetration into the dermis of the skin and then mediates oxidative stress in skin cells, ultimately producing the appearance of skin photoaging and photoinjury [4]. Photoaging can also be seen as external skin aging and includes sagging skin, increased wrinkles, dryness and patchy/mottled pigmentation, and can also cause skin cancer in severe cases [5]. The superposition of reactive oxygen species (ROS) is one of the core mechanisms of skin aging, which accumulate in large amounts under UVA irradiation, causing oxidative stress that can lead to lipid, protein, nucleic acid and organelle damage [6]. Ultraviolet irradiation induces the breakdown of the skin's connective tissue by activating matrix metalloproteinases (MMPs), and the synthesis of collagen interacts with the inhibition of MMPs, both of which are closely related to skin aging and can lead to increased wrinkles and decreased elasticity [7].

Among all probiotics, *Lactobacillus* is the best producer of exopolysaccharides, and the *Lactobacillus* family is recognized as a safe organism [8, 9]. *Lactobacillus reuteri* is widespread in the intestines of vertebrates and mammals, and can grow in both anaerobic and non-anaerobic environments. As a probiotic, it serves a variety of functions in humans, such as regulating the host immune system and intestinal microflora to relieve inflammation and maintain body homeostasis, secreting broad spectrum antibacterial compounds, regenerating and repairing host intestinal epithelial tissue, preventing diarrhea and colitis, improving cholesterol metabolism, reducing cardiovascular disease, promoting anti-allergic effects, maintaining oral health, relieving depression and reducing crying in infants and young children [10].

Numerous studies have proven that polysaccharides have antioxidant and anti-aging effects on the skin. This is because they can scavenge free radicals, improve the expression of antioxidant enzymes and inhibit the content of lipid peroxides, thereby delaying skin aging caused by ultraviolet radiation [11]. At present, research on *Lactobacillus reuteri* EPS is focused on their development and application in food, and antibacterial and anti-inflammatory effects on epithelial cells [12–14], and there is no experiment to study the *Lactobacillus reuteri* EPS protection of cells damaged by UVA irradiation. Therefore, this study focuses on cellular oxidative stress induced by UVA irradiation to explore whether *Lactobacillus reuteri* SJ-47 EPS can protect human skin fibroblasts (HSF) under UVA radiation.

We isolated a strain of *Lactobacillus reuteri* SJ-47 from yogurt in the laboratory, and its EPS showed strong antioxidant activity in vitro. We then conducted experiments on *Lactobacillus reuteri* SJ-47 EPS at the biochemical, cellular and molecular levels to further validate their cellular efficacy.

2. Materials And Methods

2.1 Materials

HSF (Cell Resource Center, Institute of Basic Medical Sciences, Chinese Academy of Medical Sciences); *Lactobacillus reuteri* SJ-47 (extracted from yogurt, deposit number: CGMCC No. 16416); Fetal Bovine Serum (FBS); Dulbecco`s Modified Eagle's Medium (DMEM); trypsin-EDTA; Phosphate Buffered Saline (PBS, Solaibao Technology, Beijing, China); penicillin-streptomycin (GIBCO Life Technologies, Grand Island, NY); Cell Counting Kit-8 (CCK8); Total Antioxidant Capacity Assay Kit with ABTS Method; Reactive Oxygen Species (ROS) Assay Kit; malondialdehyde (MDA); superoxide dismutase (SOD); catalase (CAT); Cell lysis buffer for BCA Protein Assay Kit and Total Glutathione Peroxidase (GSH-px) Assay Kit (Beyotime Biotechnology, Shanghai, China); Human Matrix Metalloproteinase-1 (MMP-1) ELISA Kit and Human Collagen-I (COL-I) ELISA Kit (CUSBIO, Wuhan, China); UElris II RT-PCR System for First-Strand cDNA Synthesis; Fast Super EvaGreen® qPCR Master Mix (Biorigin (Beijing, China) Inc).

2.2 Extraction and purification of *Lactobacillus reuteri* SJ-47 EPS

First, *Lactobacillus reuteri* SJ-47 was inoculated in MRS medium with pH 5.8–6.5,and statically incubated overnight at 37°C and 180 rpm to obtain fermentation broth, then centrifuged (8,000 rpm for 15 min at 4°C) to collect the supernatant. Concentrating the fermentation supernatant by rotary evaporation can effectively reduce the use of anhydrous ethanol. We mixed fermentation supernatant and ethanol with a volume ratio of 4:1, and samples were pelleted at -4°C for approximately 14 h. The samples were dissolved with water, 2% volume of papain was added, the two were mixed thoroughly, the reaction was carried out at room temperature for 3 h and boiled for 15 min to inactivate the papain. The precipitate was collected after the second alcohol precipitation, and crude EPS were obtained after lyophilization. Finally, we obtained *Lactobacillus reuteri* SJ-47 EPS using DEAE-52 anion column chromatography and tracking detection using the sulfuric acid-phenol method [15].

2.3 Cellular analysis of *Lactobacillus reuteri* SJ-47 EPS

2.3.1 Cell culture

The HSF used for the experiments were between 5 and 20 generations. The HSF were placed in a CO_2 incubator (Heracell™ VIOS 250i, Thermo Fisher Scientific (China) Co., Ltd.) and grown in a complete DMEM medium (containing 1% penicillin-streptomycin and 10% FBS). The medium was changed every 48 h and dissociated using 0.25% trypsin and 0.02% EDTA. All tests were carried out for 12 h after the cells were seeded at 1×10^4 cells/well in 96-well microplates (or 8×10^5 cells/well in 6-well microplates).

2.3.2 Cell viability

The HSF were seeded in a 96-well plate at 1×10^4 cells/well and grown in a complete DMEM medium, washed with PBS after 12 h and divided into the model group, blank control group and sample group. The HSF were then treated with serum-free DMEM and EPS at different concentrations (10–1,000 μg/mL) while the cells in the control group and model group were left untreated, and six parallel lines were made for each sample. After one day of culture, the HSF were induced with UVA at a total energy of 18 J/cm^2. Three other parallel samples of different concentrations were not irradiated. After UVA irradiation, the cells were again rinsed twice with PBS and freshly cultured with serum-free DMEM and EPS at different concentrations. After 12 h of incubation, 10 μL of CCK-8 solution was added, followed by incubation for 4 h and assay at 450 nm with a fluorescence microplate reader.

2.3.3 Determination of antioxidant capacity

Intracellular antioxidant levels can be measured in three parts. First, the antioxidant capacity of the cells was evaluated by assessing the intracellular free radical scavenging rate and ROS content. Second, the lipid oxidation level of cells with different EPS concentrations was judged by measuring the content of MDA in the cells. Finally, the protective effects of different concentrations of EPS on antioxidant enzymes (CAT, GSH-px and SOD) under UVA irradiation were determined. The HSF were seeded in 6-well plates at 8×10^5 cells/well and grown in a complete DMEM medium. After 12 h of incubation, the HSF were incubated with serum-free DMEM and EPS at various concentrations (100–500 μg/mL). After one day of culture, the HSF were stimulated with UVA at a total energy of 18 J/cm^2, treated twice with PBS and collected for detection. All experiments were performed according to the instructions.

2.3.4 ELISA

The contents of COL-I and MMP-1 in the cells were determined by enzyme-linked immunosorbent assay (ELISA), then an anti-aging analysis was performed. The HSF were seeded into 6-well plates at 8×10^5 cells/well and grown in a complete DMEM medium. 12 h after inoculation, the HSF were incubated with serum-free DMEM and EPS of different concentrations (100–500 μg/mL) for 24 h, then induced with UVA at a total energy of 18 J/cm^2. After 12 h of incubation, the HSF were centrifuged to collect the supernatant for detection. All experiments were performed according to the instructions.

2.4 RT-qPCR

RT-qPCR was used to measure the expression of antioxidant enzyme genes CAT, SOD and GSH-px, and anti-aging genes COL-I and MMP-1. The expression of genes related to the cell senescence and apoptosis pathways (Bax, Bcl-2, SIRT1, p16, p53, AKT, p21, FOXO) was detected by adding EPS and irradiating with UVA. The HSF were seeded in 6-well plates at 8×10^5 cells/well and grown in a complete DMEM medium. After 12 h of incubation, the HSF were incubated with serum-free DMEM and EPS (500 μg/mL) of different concentrations. After one day of culture, the HSF were induced with UVA at a total energy of 18 J/cm^2, treated twice with PBS and collected for subsequent testing. Total RNA was extracted using Trizol and the final cDNA synthesis and qPCR operations were performed using an UEIris II RT-PCR System for First-Strand cDNA Synthesis (BN12028) Inc.) and Fast Super EvaGreen® qPCR Master Mix (BN12008) respectively. The primer sequence information is shown in Table 1:

Table 1
List of Primer Sequences

Primer name	
β-actin	F: 5'-CTGAAGCCCCACTCAATCCA – 3'
	R: 5'-GCCAAGTCAAGACGGAGGAT – 3'
CAT	F: 5'-CCTTCGACCCAAGCAA-3'
	R: 5'-CGATGGCGGTGAGTGT-3'
SOD	F: 5'-TGGAGATAATACAGCAGGCT-3'
	R: 5'-AGTCACATTGCCCAAGTCTC-3'
GSH-px	F: 5'-AGAAGTGCGAGGTGAACGGT-3'
	R: 5'-CCCACCAGGAACTTCTCAAA-3'
COL-I	F: 5'- CCTGGTCCTCCTGGTAGT-3'
	R: 5'-TCCCTTCTCTCCTGGTTG-3'
MMP-1	F: 5'-TTGAGAAGCCTTCCAACTCTG-3'
	R: 5'-CCGCAACACGATGTAAGTTGTA-3'
Bax	F: 5'-CGGAATTCATGGACGGGTCCGGGGAG-3'
	R: 5'-CCGCTCGAGTCAGCCCATCTTCTTCCAG-3'
Bcl-2	F: 5'-ATGTGTGTGGAGAGCGTCAACC-3'
	R: 5'-CAGAGACAGCCAGGAGAAATCAA-3'
SIRT1	F: 5'-CAAGGGATGGTATTTATGCTCG-3'
	R: 5'-CAAGGCTATGAATTTGTGACAGAG-3'
p16	F: 5'-AGCCTTCGGCTGACTGGCTGG-3'
	R: 5'-CTGCCCATCATGACCTGG-3'
p53	F: 5'-CTTTGAGGTGCGTGTTTGTGC-3'
	R: 5'-GGTTTCTTCTTTGGCTGGGGA-3'
AKT	F: 5'-GCCGCTGCTTCTTTATCC-3'
	R: 5'-GCCATTCTCCACTCCACC-3'
p21	F: 5'-GAGGCCGGGATGAGTTGGGAGGAG-3'
	R: 5'-CAGCCGGCGTTTGGAGTGGTAGAA-3'

Primer name	
FOXO	F: 5'-TGAGGGTTAGTGAGCAGGTTAC-3'
	R: 5'-AGGGAGTTGGTGAAAGACATC-3'

2.6 Statistical Analysis

Three separate experiments with three technical replicates were performed for each sample. The results were expressed as mean ± standard deviation (Mean ± SD) by one-way analysis of variance (ANOVA) to determine which factors were significantly different. GraphPad Prism9 was used for statistical analysis. $P < 0.05$ was considered statistically significant.

3. Results

3.1 Effects of EPS on UVA-irradiated HSF cell viability

In this study, a CCK8 assay was used to determine the cytotoxicity of EPS and the protective effects of EPS addition on HSF under UVA irradiation. As shown in Fig. 1, EPS has no toxic effects on cells at concentrations between 10 and 1,000 μg/mL. At the same time, the cell activity rate increased significantly with the increase in EPS concentration, which suggests that EPS has a proliferation effect on cells. Meanwhile, cells were obviously damaged after UVA radiation and cell viability increased with the increase in EPS concentration. This phenomenon further confirmed that EPS has certain protective effects and helps to restore damage caused by UVA to HSF cells. In view of the protective effect of EPS on cells after UVA irradiation, EPS concentrations of 100, 200 and 250 μg/mL were used for subsequent tests.

3.2 Effects of EPS on ABTS, ROS and MDA in UVA-irradiated HSF cells

According to the experimental data shown in Fig. 2, EPS can reduce the oxidative stress of cells under UVA irradiation and thus alleviate oxidative damage. First, we detected the antioxidant capacity of the HSF cells (Fig. 2A), which decreased significantly after UVA irradiation. With the increase in EPS concentration, the antioxidant capacity of the cells increased, presenting an apparent dose-dependent relationship. Afterwards, the ROS content in the HSF cells was detected (Fig. 2B), and it was found that ROS increased significantly after UVA irradiation. Treating HSF with EPS can reduce the content of ROS produced under UVA irradiation, and the ROS content can be basically restored to the same level as that of the control group. Cellular oxidative stress was accompanied by lipid oxidation, and the degree of lipid oxidation was judged by measuring the MDA content (Fig. 2C). The MDA content was significantly decreased in HSF treated with EPS.

3.3 Effects of EPS on CAT, SOD and GSH-px activity in UVA-irradiated HSF cells

CAT, SOD and GSH-px are common antioxidant enzymes in the antioxidant system of cells. Antioxidant enzymes protect the organelles from oxidative damage by removing free radicals and ROS produced in cells. As shown in Fig. 3A, the CAT content in cells decreased significantly after UVA irradiation, while EPS could weaken the trend of CAT decline in HSF cells. Combined with Fig. 3D, it can be seen that EPS could induce HSF cells to increase the expression of CAT mRNA in an obvious dose-dependent relationship. It can be seen from Fig. 3B and Fig. 3E that the SOD content in cells decreased significantly after UVA irradiation. When the EPS concentration was 500 μg/mL, the relative expression of SOD mRNA in the cells was significantly increased, and the SOD content in the cells was also increased. It can be seen from Fig. 4C that the GSH-px content in cells was significantly reduced after UVA irradiation, and when the EPS concentration was 500 μg/mL, the GSH-px content was significantly increased ($P < 0.001$). As can be seen from Fig. 4F, the GSH-px mRNA expression level was significantly increased under different concentrations of EPS. In conclusion, EPS can promote the increase of the mRNA relative expression level of antioxidant enzymes in HSF after UVA irradiation and repair oxidative stress damage by increasing the activity of CAT, SOD and GSH-px.

3.4 Effects of EPS on UVA-irradiated COL-I and MMP-1 contents

A major factor in skin aging is the loss of collagen and the degradation of the extracellular matrix, while the latter can affect the synthesis of collagen. In this study, COL-I and MMP-1 contents and mRNA relative expression levels were measured to evaluate whether EPS had a certain delaying effect on cell senescence. It can be seen from Fig. 4A, the content of COL-I in HSF was significantly reduced. Under UVA irradiation after EPS pretreatment, the content of COL-I in HSF was significantly increased in a dose-dependent manner. It can be seen from Fig. 4C, EPS obviously increased the mRNA expression level of COL-I in UVA-induced cells. This indicates that EPS can promote the generation of collagen after oxidative stress. As shown in Fig. 4B that the content of cell matrix metalloenzyme increased significantly after UVA irradiation, indicating that oxidative stress can promote the accelerated degradation of the extracellular matrix, while EPS can inhibit the generation of MMP-1. Combined with Fig. 4D, it can be seen that when the concentration of EPS was 500 μg/mL, MMP-1 mRNA expression was significantly decreased ($P < 0.001$). In conclusion, EPS can improve premature aging caused by UVA irradiation and delay skin aging.

3.5 Effects of EPS on UVA-irradiated cell senescence and apoptosis pathways

Based on the above experimental data, we finally chose to detect the mRNA relative expression levels of the HSF senescence and apoptosis pathways after UVA irradiation when the EPS concentration was 500 μg/mL. It can be seen from Fig. 5A that the relative expression level of Bax mRNA in HSF cells was up-regulated after UVA irradiation, while it was significantly down-regulated and obviously lower than that of the control group after EPS pretreatment. It can be seen from Fig. 5B, the relative expression level of Bcl-2 mRNA in HSF was down-regulated after UVA irradiation, while it was significantly up-regulated after EPS

pretreatment to 2.7 times that of the control group. As can be seen from Fig. 5C that the relative expression level of SIRT1 mRNA in HSF was down-regulated after UVA irradiation, while it was significantly up-regulated and obviously higher than that of the control group after EPS pretreatment. It can be seen from Fig. 5D, the relative expression level of p16 mRNA in HSF cells was obviously up-regulated after UVA irradiation, while it was significantly down-regulated after EPS pretreatment and obviously lower than that of the control group. It can be seen from Fig. 5E, the relative expression level of p53 mRNA in HSF cells was up-regulated after UVA irradiation, while it was down-regulated after EPS pretreatment to 0.4 times that of the control group. Figure 5F shows that the relative expression level of AKT mRNA in HSF cells was down-regulated after UVA irradiation, while it was significantly up-regulated after EPS pretreatment. As can be seen from Fig. 5G, the relative expression level of p21 mRNA in HSF cells was down-regulated after UVA irradiation, while it was significantly up-regulated after EPS pretreatment to four times that of the control group. As can be seen from Fig. 5H, the relative expression level of FOXO mRNA in HSF cells was significantly up-regulated after UVA irradiation, while it was significantly down-regulated after EPS treatment. In conclusion, when the EPS concentration was 500 μg/mL, the expression of key genes in the UVA-induced HSF cell senescence and apoptosis pathways was regulated to repair the oxidative stress damage to cells.

4. Discussion

Transcription factor forkhead box protein O (FOXO) is a downstream effector of AKT, and the expression of FOXO target genes regulates cell growth, apoptosis and senescence [16]. FOXO is phosphorylated and degraded by AKT [17], and the inhibition of AKT phosphorylation in the presence of apoptotic factors facilitates the translocation of dephosphorylated FOXO into the nucleus and triggers the expression of apoptosis-related genes (Bax, p16, p21 and p53, etc.), which leads to cell growth cycle arrest and apoptosis [18–21]. Among them, the p21 gene can resist apoptosis, and at the same time it inhibits proliferation and promotes apoptosis. On the one hand, p21 can cause cell cycle arrest, giving cells extra time to repair damage; on the other hand, p21 upregulation promotes apoptosis, so it has an antagonistic duality [21]. However, SIRT1 can inhibit the expression of apoptotic factors through the deacetylation of p53 and FOXO, and promote the expression of genes related to cell damage repair and growth (SOD, CAT and Bcl-2, etc.) [22, 23].

According to other studies, excessive UV radiation promotes phenomena such as apoptosis and stress damage, which lead to skin aging. To investigate and analyze the value of *Lactobacillus reuteri* SJ-47 EPS in skin protection, a UVA-induced HSF model was established to investigate the oxidative stress protective and anti-aging effects of EPS on HSF at the biochemical, cellular and molecular levels, and our findings are consistent with this conclusion. The down-regulation of AKT and SIRT1 expression and up-regulation of FOXO expression in HSF under UVA stimulation at 18 J/cm2 indicated the activation of the FOXO apoptotic pathway. This was evidenced by the marked up-regulation of the expression levels of downstream pro-apoptotic factors Bax, p16 and p53. Fortunately, the level of the activated FOXO apoptotic pathway was extremely significantly decreased in EPS-treated HSF when they were stimulated by UVA again. In particular, the expression levels of AKT, SIRT1 and anti-apoptotic factor Bcl-2 were

extremely significantly up-regulated, which largely inhibited the nuclear displacement and acetylation levels of FOXO, thereby reducing the expression of apoptotic factors, while the up-regulation of p21 causes cell cycle arrest to repair cell damage, and ultimatesly promotes cell growth and oxidative stress repair, as evidenced by the increased activity and expression levels of cellular antioxidant enzymes and increased cell survival rate. For example, under UVA stimulation, the survival rate of HSF incubated with EPS increased to 64% from 32% without incubation, while the intracellular antioxidant enzymes (SOD, CAT and GSH-px) showed a significant increase in enzyme activity and expression level. Under the incubation of 500 μg/mL EPS, the antioxidant capacity of cells was significantly increased, and the contents of ROS and MDA were obviously decreased. In addition, we found that the expression of MMP-1 in HSF after EPS incubation was inhibited and the corresponding enzyme activity was significantly reduced, while the expression level of Type I procollagen and extracellular COL-I content were significantly up-regulated, all of which resulted in the optimal effects of EPS at 500 μg/mL, effectively alleviating skin aging caused by the degradation of the extracellular matrix due to UVA irradiation.

In conclusion, *Lactobacillus reuteri* SJ-47 EPS have strong photoprotective effects on UVA-irradiated HSF, giving them great significance in the regulation of the cell senescence and apoptosis pathways, and great potential value in cosmetic applications. However, further experiments are required to analyze the single components of *Lactobacillus reuteri* SJ-47 EPS and explore their physical and chemical properties. At the same time, in addition to the antioxidant effects of *Lactobacillus reuteri* SJ-47 EPS, we can also study their other effects on cells and further determine whether EPS can become a functional raw material for cosmetics.

Abbreviations

EPS: Lactobacillus reuteri SJ-47 exopolysaccharides

HSF: human skin fibroblasts

ROS: reactive oxygen species

MDA: malondialdehyde

MMPs: matrix metalloproteinases

FBS: Fetal Bovine Serum

DMEM: Dulbecco`s Modified Eagle's Medium

PBS: Phosphate Buffered Saline

CCK8: Cell Counting Kit-8

SOD: superoxide dismutase

CAT: catalase

GSH-px: Glutathione Peroxidase

MMP-1: Matrix Metalloproteinase-1

COL-I: Human Collagen-I

ELISA: enzyme-linked immunosorbent assay

FOXO: Transcription factor forkhead box protein O

Declarations

Ethics approval and consent to participate

Not applicable.

Consent for publication

Not applicable.

Availability of data and materials

The datasets used during the current study are available from the corresponding author on reasonable request.

Competing interests

The authors declare that they have no competing interests.

Funding

This study was supported by the Research Foundation for Youth Scholars of Beijing Technology and Business University.

Authors' contributions

Meng Li and Yongtao Zhang modified the format of the article, Jingsha Zhao, Dongdong Wang and Jiachan Zhang sorted out the data, Meng Li, Dan Zhao and Hao Fu designed the Experiment, Hao Fu and Yongtao Zhang carried out the main experiments and performed data analyses, Jingsha Zhao, Meng Li and Changtao Wang finally wrote and summarized the text. The authors read and approved the final manuscript.

Acknowledgements

The authors thank College of Chemistry and Materials Engineering, Beijing Technology and Business University.

References

1. Feng, Chen et al (2019) 6-shogaol, a active constiuents of ginger prevents UVB radiation mediated inflammation and oxidative stress through modulating NrF2 signaling in human epidermal keratinocytes (HaCaT cells). J Photochem Photobiology B: Biology 111518. 197doi:10.1016/j.jphotobiol.2019.111518
2. Gail Jenkins (2002) Molecular mechanisms of skin ageing. Mech Ageing Dev 123(7):801–810. doi:10.1016/S0047-6374(01)00425-0
3. Debacq-Chainiaux, Florence et al (2012) UV, stress and aging.. Dermato-endocrinology, 4(3), pp. 236 – 40. doi:10.4161/derm.23652
4. Polefka Thomas G et al (2012) Effects of solar radiation on the skin. J Cosmet Dermatol 11(2):134–143. doi:10.1111/j.1473-2165.2012.00614.x
5. Hseu Y-C et al (2019) Zerumbone Exhibits Antiphotoaging and Dermatoprotective Properties in Ultraviolet A-Irradiated Human Skin Fibroblast Cells via the Activation of Nrf2/ARE Defensive Pathway.. Oxidative medicine and cellular longevity, 2019pp. 4098674. doi:10.1155/2019/4098674
6. Yanpei, Gu et al (2020) Biomarkers, oxidative stress and autophagy in skin aging. Ageing Research Reviews, 59(prepublish), pp. 101036. doi:10.1016/j.arr.2020.101036
7. Jung-Ae, Kim et al (2012) Chitooligomers inhibit UV-A-induced photoaging of skin by regulating TGF-β/Smad signaling cascade. Carbohydr Polym 88(2):490–495. doi:10.1016/j.carbpol.2011.12.032
8. Petra, Kšonžeková et al (2016) Exopolysaccharides of Lactobacillus reuteri: Their influence on adherence of E. coli to epithelial cells and inflammatory response. Carbohydr Polym 141:10–19. doi:10.1016/j.carbpol.2015.12.037
9. Jyotsna J et al (2014) Biosynthesis of 1,3-propanediol from glycerol with Lactobacillus reuteri: Effect of operating variables. J Biosci Bioeng 118(2):188–194. doi:10.1016/j.jbiosc.2014.01.003
10. Mu Qinghui and Tavella, Vincent J, Luo Xin M (2018) Role of Lactobacillus reuteri in Human Health and Diseases.. Frontiers in microbiology, 9pp. 757. doi:10.3389/fmicb.2018.00757
11. Sun, Qianru et al (2021) Protective effects of LPL-EPS-02 on human dermal fibroblasts damaged by UVA radiation. J Funct Foods 83. doi:10.1016/J.JFF.2021.104544
12. Tharani Shanmugam and Bharathi Devaraj and, Ranjithkumar R (2020) Extracellular green synthesis of chitosan-silver nanoparticles using Lactobacillus reuteri for antibacterial applications. Biocatal Agric Biotechnol 101838. 30doi:10.1016/j.bcab.2020.101838
13. Hümeyra İspirli et al (2019) Physicochemical characterisation of an α-glucan from Lactobacillus reuteri E81 as a potential exopolysaccharide suitable for food applications. Process Biochem 79:91–96. doi:10.1016/j.procbio.2018.12.015

14. Éile Butler and Christoffer Lundqvist and Jakob Axelsson (2020) Lactobacillus reuteri DSM 17938 as a Novel Topical Cosmetic Ingredient: A Proof of Concept Clinical Study in Adults with Atopic Dermatitis. Microorganisms 8(7). doi:10.3390/microorganisms8071026
15. Michel, DuBois et al (2002) Colorimetric Method for Determination of Sugars and Related Substances. Anal Chem 28(3):350–356. doi:10.1021/ac60111a017
16. Hou Y-Q et al (2016) Juglanthraquinone C Induces Intracellular ROS Increase and Apoptosis by Activating the Akt/Foxo Signal Pathway in HCC Cells. Oxidative Medicine and Cellular Longevity, 2016pp. 4941623. doi:10.1155/2016/4941623
17. Hartmann W et al (2009) Activation of phosphatidylinositol-3'-kinase/AKT signaling is essential in hepatoblastoma survival. Clin cancer research: official J Am Association Cancer Res 15(14):4538–4545. doi:10.1158/1078-0432.CCR-08-2878
18. Orabi Sahar, Hassan et al (2020) The Antioxidant, Anti-Apoptotic, and Proliferative Potency of Argan Oil against Betamethasone-Induced Oxidative Renal Damage in Rats. Biology 9(11). doi:10.3390/BIOLOGY9110352
19. Wang Zhixue and Fang Jifeng and Xiao Jizhou (2019) Correlation of the expression of inflammatory factors with expression of apoptosis-related genes Bax and Bcl-2, in burned rats. Experimental and therapeutic medicine 17(3):1790–1796. doi:10.3892/etm.2018.7118
20. Laurence J et al (2019) Atrial Fibrillation Progression Is Associated with Cell Senescence Burden as Determined by p53 and p16 Expression. J Clin Med 9(1):36–36. doi:10.3390/jcm9010036
21. Geena Mariya Jose and, Muraleedhara Kurup G (2017) Sulfated polysaccharides from Padina tetrastromatica arrest cell cycle, prevent metastasis and downregulate angiogenic mediators in HeLa cells. Bioactive Carbohydr Diet Fibre 7–13. 12doi:10.1016/j.bcdf.2017.10.001
22. Liu, XiaoHu et al (2021) Ginsenoside Rg1 attenuates premature ovarian failure of D-gal induced POF mice through downregulating p16INK4a and upregulating SIRT1 expression.. Endocrine, metabolic & immune disorders drug targets. 10.2174/1871523020666210830164152
23. Chen L et al (2019) 1,25-Dihydroxyvitamin D exerts an antiaging role by activation of Nrf2-antioxidant signaling and inactivation of p16/p53-senescence signaling. Aging Cell 18(3):e12951. doi:10.1111/acel.12951

Figures

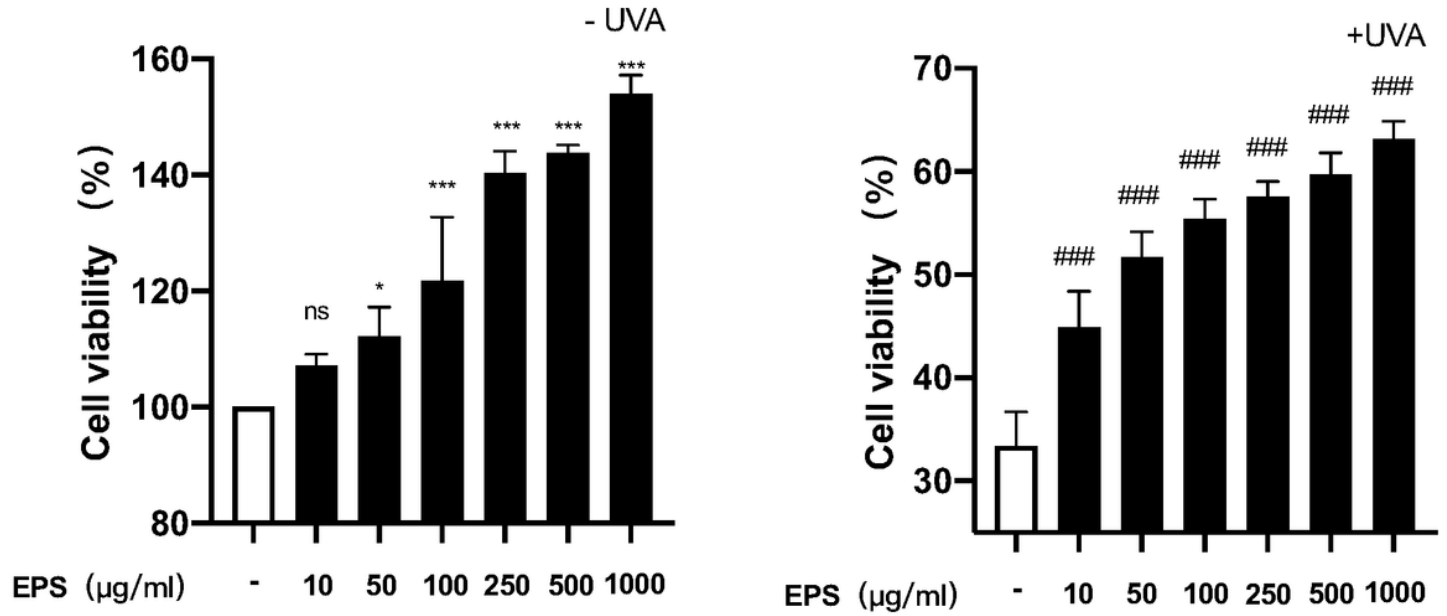

Figure 1

Effects of different concentrations of EPS on HSF survival rate under normal conditions and after UVA irradiation. *p < 0.05, **p < 0.01, ***p < 0.001 compared to untreated control group; #p < 0.05, ##p < 0.01, ###p < 0.001, compared to model group

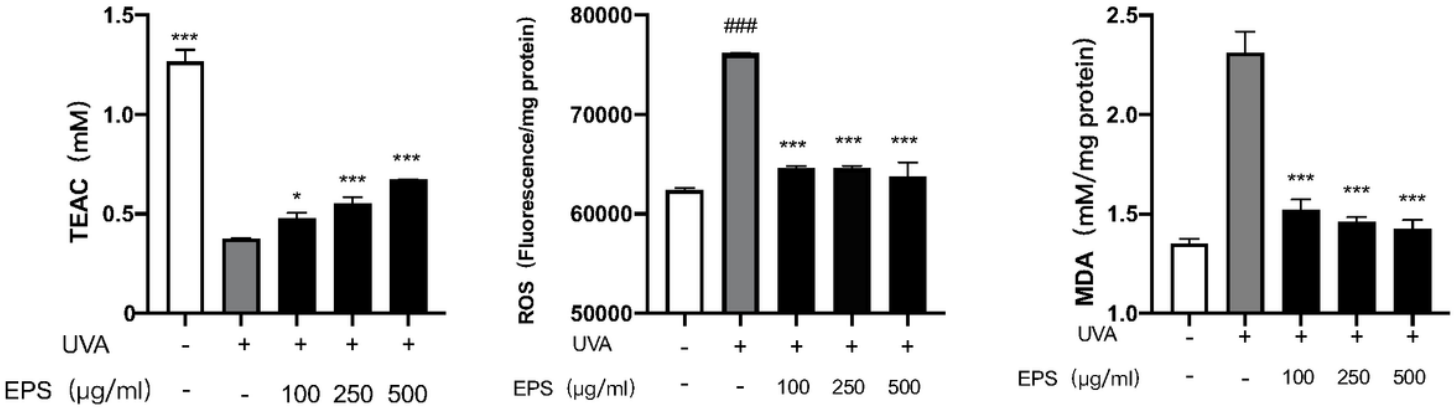

Figure 2

Effects of different concentrations of EPS on total antioxidant capacity (ABTS), ROS scavenging capacity and MDA content: (A) Determination of Trolox Equivalent Antioxidant Capacity (TEAC) under UVA

irradiation; (B) Fluorescence intensity of HSF under UVA irradiation; (C) Malondialdehyde content of HSF under UVA irradiation. *p < 0.05, **p < 0.01, ***p < 0.001 compared to model group

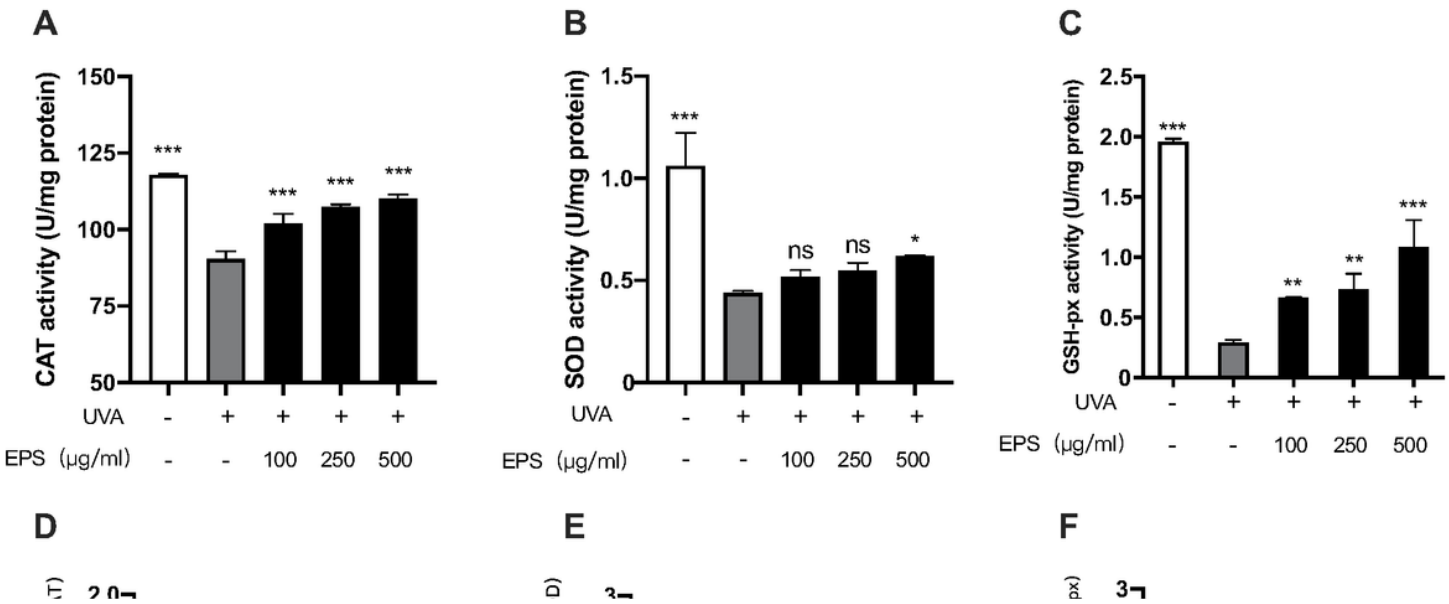

Figure 3

Effects of different concentrations of EPS on antioxidant enzymes CAT (A), SOD (B) and GSH-px (C) in HSF under UVA irradiation. Relative mRNA expression levels of CAT (D), SOD (E) and GSH-px (F) under UVA irradiation after treatment with different concentrations of EPS. Each mRNA was referenced to the internal control gene β-actin and expressed relative to the control group. *p < 0.05, **p < 0.01, ***p < 0.001 compared to model group

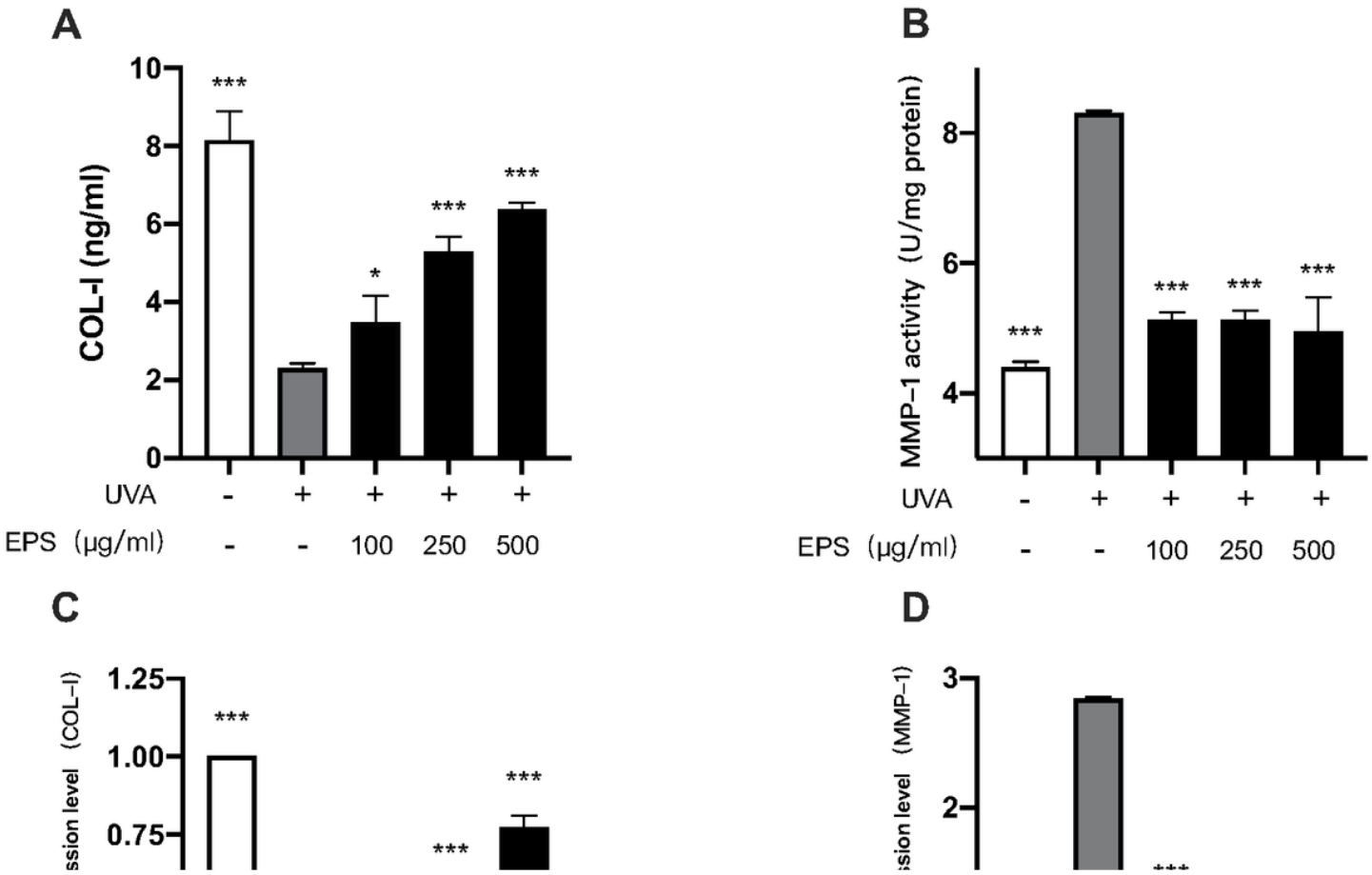

Figure 4

Effects of different concentrations of EPS on COL-I (A) and MMP-1 (B) in HSF under UVA irradiation. Relative expression levels of COL-I (C) and MMP-1 (D) mRNA in HSF under UVA irradiation with different concentrations of EPS. Each mRNA was referenced to the internal control gene β-actin and expressed relative to the control group. *p < 0.05, **p < 0.01, ***p < 0.001 compared to model group

Figure 5

Effects of different concentrations of EPS on the expression of key genes in the HSF senescence and apoptosis pathways induced by UVA. Each mRNA was referenced to the internal control gene β-actin and expressed relative to the control group. *p < 0.05, **p < 0.01, ***p < 0.001 compared to model group

Supplementary Files

This is a list of supplementary files associated with this preprint. Click to download.

- GraphicalAbstract.pdf